Neuron, Volume *104*

Supplemental Information

Targeted Cortical Manipulation of Auditory Perception

Sebastian Ceballo, Zuzanna Piwkowska, Jacques Bourg, Aurélie Daret, and Brice Bathellier

Supplementary Figures
Ceballo et al., 2019

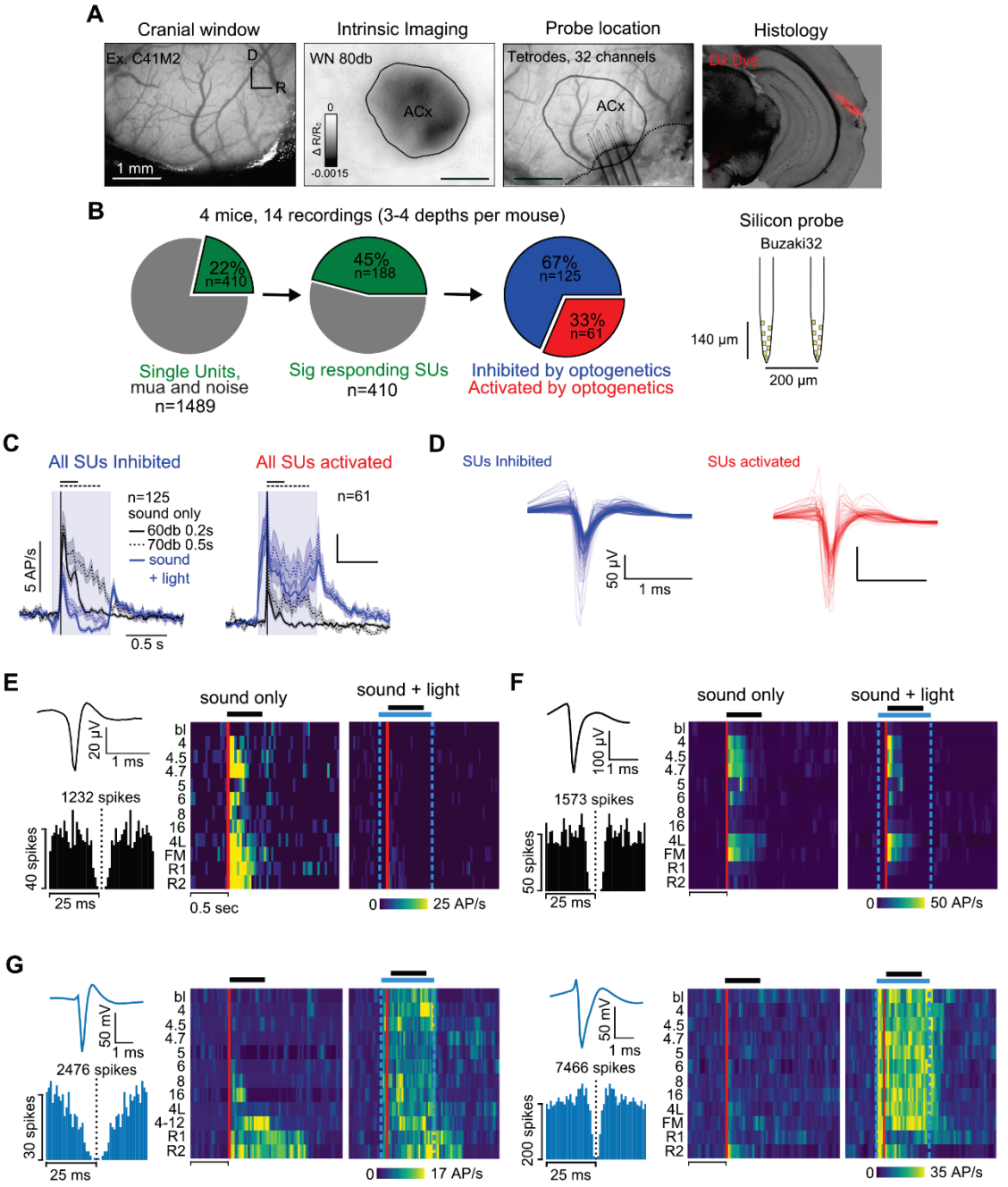

Figure S1, related to Fig. 2| PV interneuron activation strongly perturbs AC responses to sounds

A. To localize AC during calibration experiments, the white noise intrinsic imaging response map (middle left), was used to target probe insertion. The cover slip of the window was slightly broken and removed, allowing the insertion of the probe into the exposed brain (middle right, see dashed line indicating glass border). At the end of the recording, the animal was perfused, and histology was done to track probe location and depth using fluorescent dye DiI. **B.** Left, Fraction of single units identified as spike clusters obtained using the KlustaKwik spike sorting algorithm which displays a clear refractory period in their spike train autocorrelogram (examples in **E-G**). Middle, Fraction of single units that significantly

respond to sounds (see *Methods*). Right, Fraction of sound-responsive cells that are activated (red) or inhibited (blue) by light-gated PV activation. **C.** Time course of mean firing rate across all single units in response to PTs of 0.2s at 60 db (black line) and to the 0.5s long 4 kHz and 4-12 kHz chirp at 70 dB (black dashed line). In blue are shown the responses to the same sound groups but during PV interneuron activation. **D.** Spike waveforms of all inhibited (blue) and activated (red) single units by the optogenetic PV+ neuron activation. Sharper waveforms, with a rapid and marked rebound after the peak of the spike were observed in activated cells and much less in inhibited cells, indicating that the expected waveform signature of PV+ cells are present in this pool of units. However, some activated units (with smaller spike amplitude) had a slow spike waveform which could be due to temporal filtering of the waveform in the tissue at long distance and/or network effects activating cells with broader spikes. **E.** Example of a single unit for which sound responses were inhibited by light. Left, Mean spike waveform (electrode site with largest amplitude) and spike train autocorrelogram for the same unit. Right, Heat map of mean firing rate in response to sounds (average over 10 trials for each sound) during sound and sound + light trials. The solid red line corresponds to sound onset. Dashed blue lines correspond to light onset and offset. **F**. Same as E but for a cell which was not inhibited by the optogenetic activation protocol. **G**. Same as E and F, but for two different cells which were activated, presumably PV-interneurons.

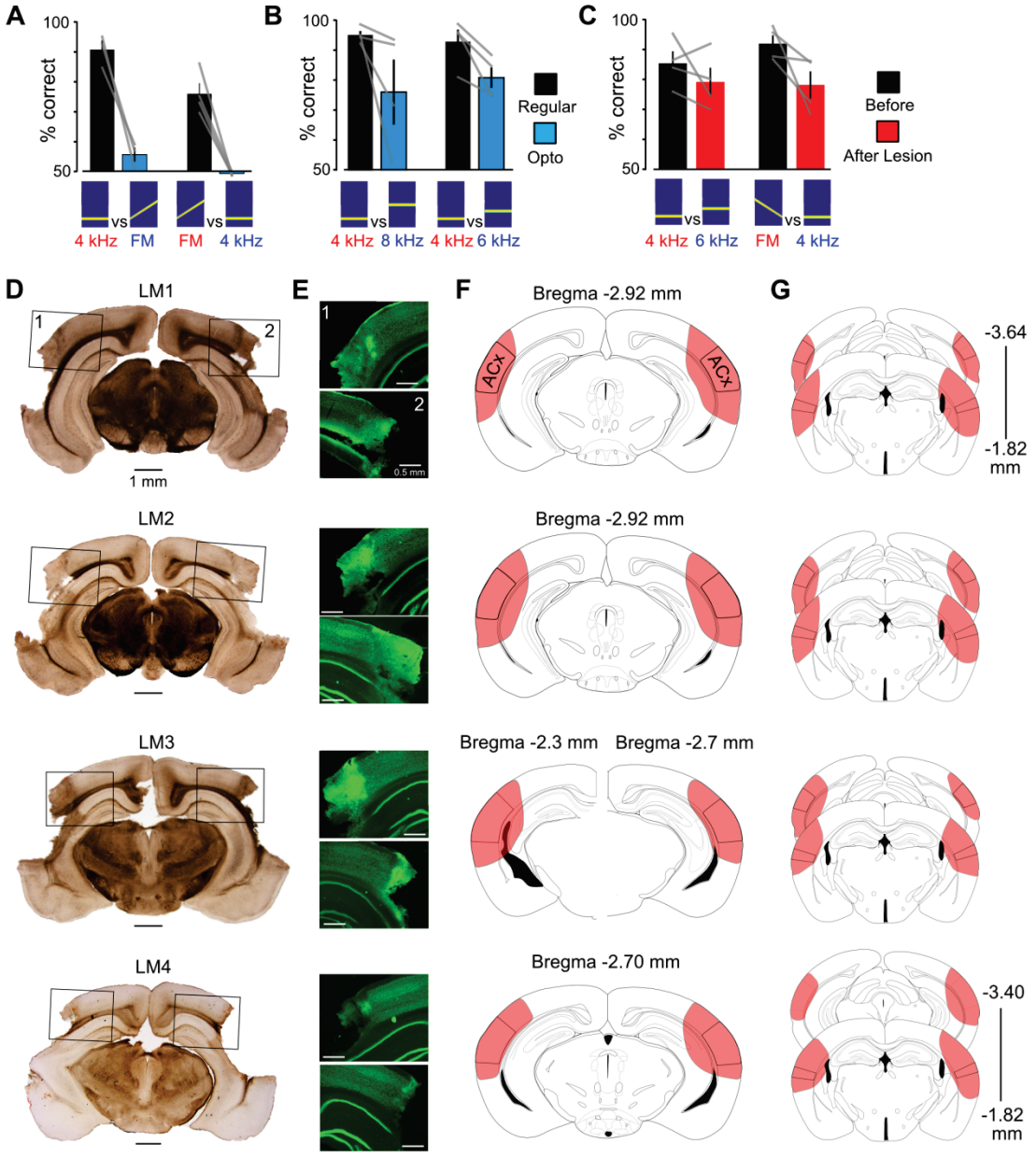

Figure S2, related to Fig. 2 | Extent of auditory cortex lesions and AC inactivations for further sound pairs

A. Mean discrimination performance without (black) and with (blue) optogenetic inactivation of AC during the FMvsPT task when the 4 kHz tone is the rewarded sound (left, 91 ± 3% vs 56 ± 2%, n = 3 mice, p =0.049, Wilcoxon rank-sum test) or when the 4-12kHz FM sweep is the S+ sound (right, 76 ± 4% vs 49 ± 0.3%, n = 4 mice, p = 0.02, Wilcox on rank-sum test) in mice expressing ChR2 in PV+ interneurons. **B**. Mean discrimination performance without (black) and with (blue) optogenetic inactivation of AC during the PTvsPT task when the 4 kHz tone is the rewarded sound and when the non-rewarded sound is an 8 kHz tone (left, 95 ± 1.3% vs 76 ± 11%, n = 4 mice, p = 0.04, Wilcoxon rank-sum test) or when the non-rewarded sound is a 6 kHz tone (right, 92 ± 3.9% vs 80 ± 3.3%, n = 4 mice, p = 0.08, Wilcoxon rank-sum test) in mice expressing ChR2 in PV+ interneurons. **C**. Mean discrimination performance

of 4 kHz versus 6 kHz pure tones before and after AC lesions (left 85 ± 3.9% vs 79 ± 4.7%, n = 4 mice, p = 0.25, Wilcoxon rank-sum test) or when a decaying FM sweep from 12-4 kHz is discriminated from a 4 kHz pure tone (92 ± 2.7% vs 78 ± 4.5%, n = 4 mice, p = 0.02, Wilcoxon rank-sum test). **D.** Bright-field images of coronal brain slices showing the extent of bilateral lesions for the four animals shown in **Figure 2G**. **E.** Epifluorescence images of identified cortical neurons (NeuN staining) for the two areas delimited by the black squares in D**.** Punctate NeuN staining indicates intact cell bodies outside of the lesion. The absence of a punctate pattern on the tissue bordering the lesion indicates that the cortical network was damaged in this zone, which was thus included into the lesioned area in our quantification. **F.** Coronal slide reconstruction modified from the Paxinos mouse brain atlas showing the location and extent of the lesion (red shading) with respect to AC (more intense black contour) at the anteroposterior location corresponding to the center of AC along this axis. The anteroposterior coordinates from bregma and AC location are indicated for each section. **G.** Same as F but for the anteroposterior locations corresponding to anterior and posterior limits of AC. Overall our reconstructions show that primary and secondary auditory cortex were fully lesioned in all four animals.

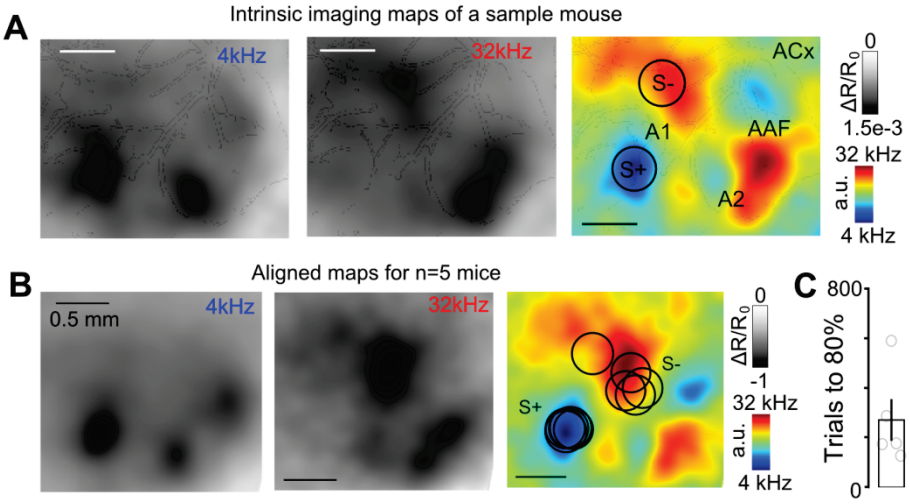

Figure S3, related to Fig. 4 | Discriminated artificial optogenetic stimuli were located in similar tonotopic locations across mice.

A. Intrinsic imaging response maps to 4 kHz and 32 kHz pure tones, on the right the main tonotopic fields are revealed by plotting the difference of 4 kHz and 32 kHz response maps. A1; primary auditory cortex, A2; secondary auditory cortex, AAF; anterior auditory field. UF; ultrasonic field. Circles correspond to the optogenetic stimulus locations shown used to drive artificial discrimination behavior in this mouse**. B.** Aligned intrinsic imaging responses to 4 kHz and 32 kHz pure tones averaged across five mice. The resulting difference map is shown on the right. The optogenetic stimulus locations for the same five animals are superimposed as black circles. **C.** Mean number of trials to reach 80% performance. Empty circles correspond to single animals and the bars to mean and SEM.

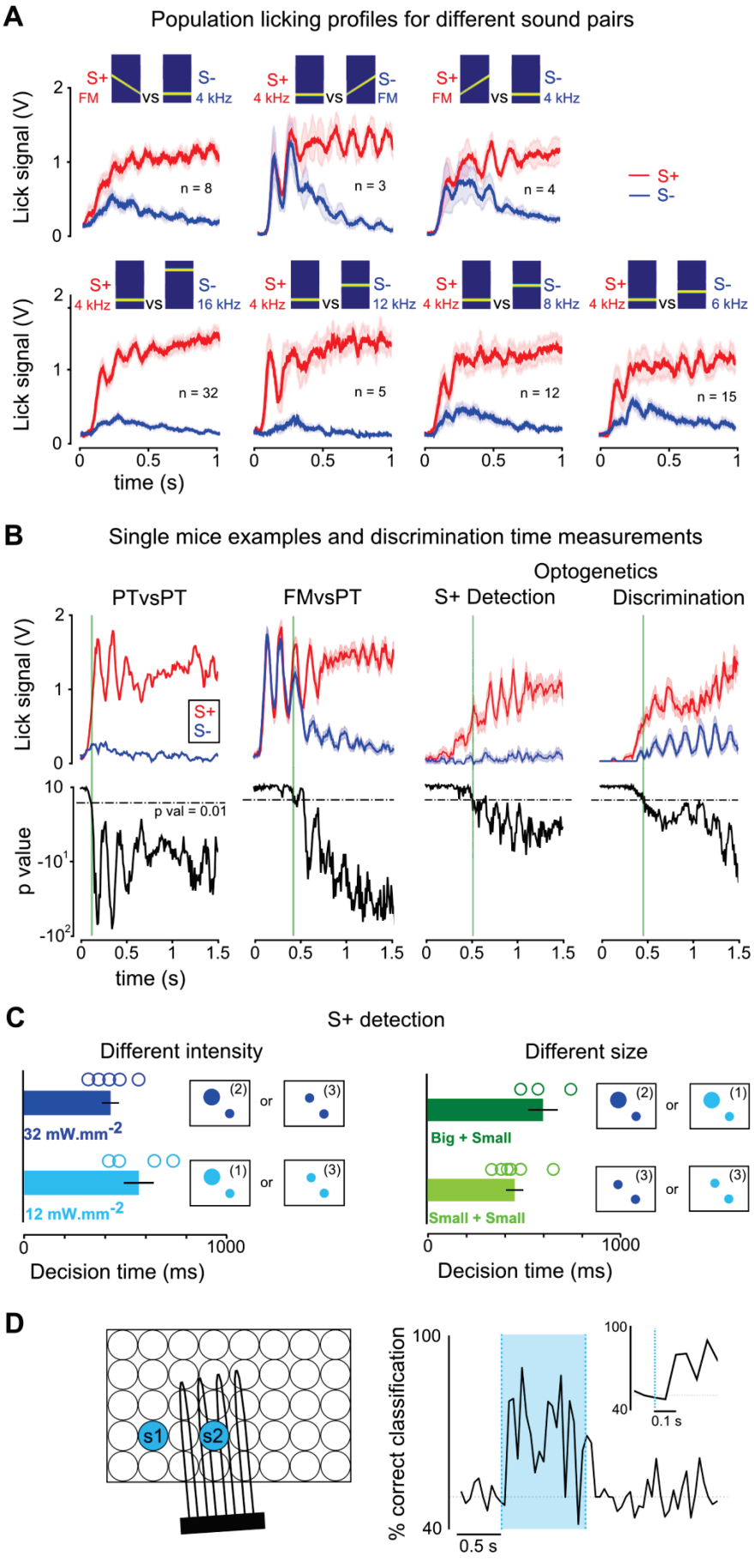
A
Population licking profiles for different sound pairs
S+ FM vs S- 4 kHz
S+ 4 kHz vs S- FM
S+ FM vs S- 4 kHz
S+ 4 kHz vs S- 16 kHz
S+ 4 kHz vs S- 12 kHz
S+ 4 kHz vs S- 8 kHz
S+ 4 kHz vs S- 6 kHz
Lick signal (V)
n = 8
n = 3
n = 4
n = 32
n = 5
n = 12
n = 15
S+
S-
time (s)
B
Single mice examples and discrimination time measurements
PTvsPT
FMvsPT
Optogenetics
S+ Detection
Discrimination
Lick signal (V)
p val = 0.01
p value
time (s)
C
S+ detection
Different intensity
32 mW.mm-2
12 mW.mm-2
Decision time (ms)
Different size
Big + Small
Small + Small
Decision time (ms)
D
s1
s2
% correct classification
0.5 s
0.1 s

Figure S4, related to Fig. 4 | Reaction time for detection of a single focal cortical stimulus is similar to discrimination time for choosing between two focal cortical stimuli. **A.** Time course of averaged lick traces for the S+ (red) and S- (blue) stimuli for seven different groups of mice performing a discrimination of the corresponding pair of stimuli. On the upper row, first column, it can be seen that if the FM sweep (S+) does not start at the same frequency as the pure tone (S-) non-discriminative licking at sound onset is greatly diminished, contrary to the hard FMvsPT task independent of the valence of the stimuli (upper row, 2nd and 3rd columns). On the lower row it can be seen that discrimination time is largely independent on frequency similarity in a pure tone discrimination, although more similar frequencies produce more incorrect licks on the S- sound. The n in each panel indicates the number of mice pooled in the analysis. **B**. Top, Time course of averaged lick traces for each stimulus in one example mouse for the two sound discrimination tasks and for detection and discrimination of optogenetic stimuli. Bottom, p-values for the null hypothesis that S+ and S- lick signals come from the same distribution obtained for every time point (Wilcoxon rank-sum test). Green lines indicate the first significant time point corresponding to discrimination time. **C.** Reaction times of 8 mice for the detection of an optogenetic stimulus of different intensities (left, 12 *vs* 32 mW.mm^{-2}) or of different sizes (right, two small disk vs one small disk + one large disk of doubled diameter). Dark blue: 32 mW.mm^{-2} (n= 4 mice). Light blue: 12 mW.mm^{-2} (n= 4 mice). Dark green: larger stimulus(n= 3 mice). Light green: smaller stimulus(n= 5 mice). **D.** Left, Sketch of the silicon probe location and grid indicating the two spots used to train an SVM classifier. Right, Performance of an SVM classifier trained for each time bin of 50 ms to discriminate between single unit population responses (n=8 neurons showing significant spatially modulated optogenetic activation for light intensity 12mW/mm^{-2}) of two optogenetic stimulations separated by approximately same distance as optogenetics stimuli used to train mice during the discrimination task (~800 µm; stimuli used are the location of peak response for each neuron and another ~800 µm distant location). The classifier was trained with a subset of 5 trials and tested on 5 different trials. Inset shows a magnification around stimulus onset indicating that discrimination is achieved between 50 and 100 ms from stimulus onset.

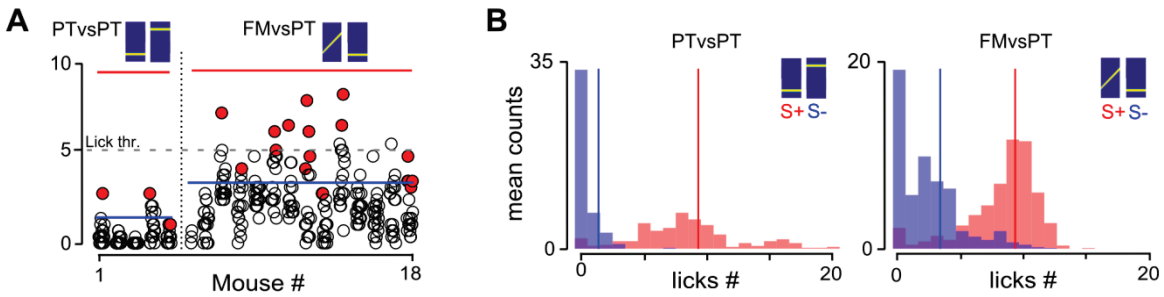

Figure S5, related to Fig. 5 | Absolute lick counts for focal optogenetic AC activation experiments and lick count distributions. **A.** Absolute mean lick counts for all optogenetic stimulus locations and all mice involved in the PTvsPT or FMvsPT tasks, as shown in a normalized version in **Figure 5E**. Red filled circles correspond to significant locations ($P < 0.05$). The blue lines indicate average lick counts for S- trials across all animals in the same task. The dashed line indicates the lick threshold for correct performance. **B.** Left, distribution of lick counts for the regular S+ and S- trials for the PTvsPT task (5 mice, same animals as in **A**) computed over 100 random trials. Right, same as left but for the FMvsPT task (13 mice, same animals as in **A**). The red and blue line indicate average lick counts for S+ and S- trials respectively (PTvsPT S+ = 9,2 and S- = 1.4 ; FMvsPT S+ = 9.2 and S- = 3.2 licks).

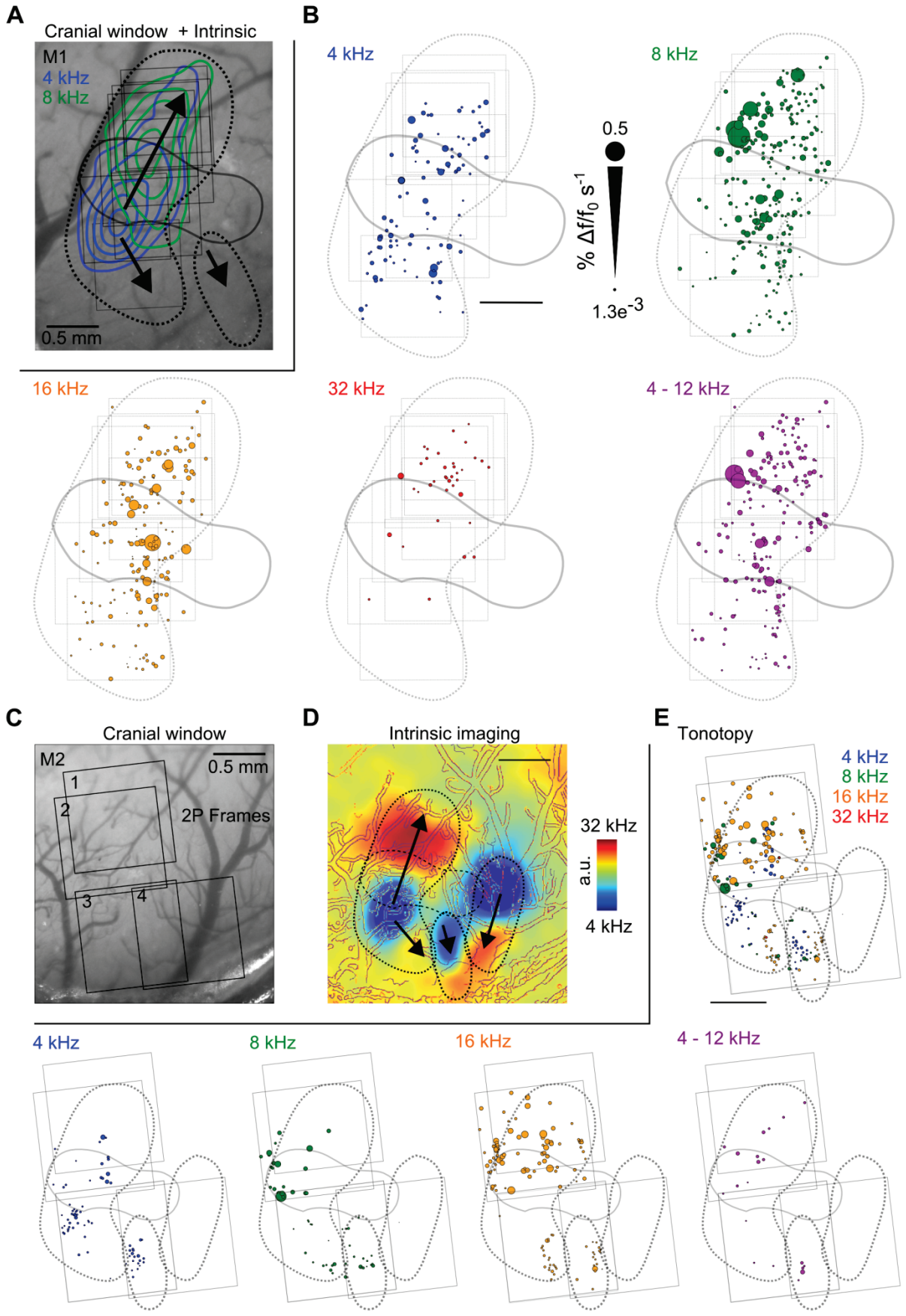
A
Cranial window + Intrinsic
M1
4 kHz
8 kHz
0.5 mm
B
4 kHz
8 kHz
0.5
% Δf/f0 s-1
1.3e-3
16 kHz
32 kHz
4 - 12 kHz
C
Cranial window
M2
0.5 mm
1
2
3
4
2P Frames
D
Intrinsic imaging
32 kHz
a.u.
4 kHz
E
Tonotopy
4 kHz
8 kHz
16 kHz
32 kHz
4 kHz
8 kHz
16 kHz
4 - 12 kHz

Figure S6, related to Fig. 6 | Tonotopic maps from intrinsic and two-photon calcium imaging are similar

A. Auditory cortex surface and localization of 2P calcium imaging field-of-view (light grey). Contour of intrinsic imaging responses to pure tones (4 kHz in blue and 8 kHz in green) and approximate tonotopics gradients (A1 and A2) obtained from mean intrinsic imaging responses of 12 mice showed in **Figure 6A** (dashed black lines). Area of optogenetic stimulation that elicited behavioral responses showed in Figure 5H (black line).

B. 2P calcium imaging responses in same animal presented in A. Neurons displayed presented significant responses (Wilcoxon rank sums pval <0.01) to pure tones. Circles diameters are proportional to the mean deconvolved calcium response over 20 repetitions. **C.** Auditory cortex surface and localization of 2P calcium imaging field-of-view of another example mouse (light grey). **D.** Tonotopic gradients obtained by subtraction of the 4 and 32 kHz intrinsic response maps. **E.** Top, 2P calcium imaging responses of field-of-views in C. Circles correspond to the localization of all significantly responding neurons. Color-code correspond to their preferred frequency over the same sounds used during intrinsic imaging experiments and size proportional to the mean deconvolved calcium response over 20 repetitions. Bottom, Same representation of 2P calcium imaging responses as B.

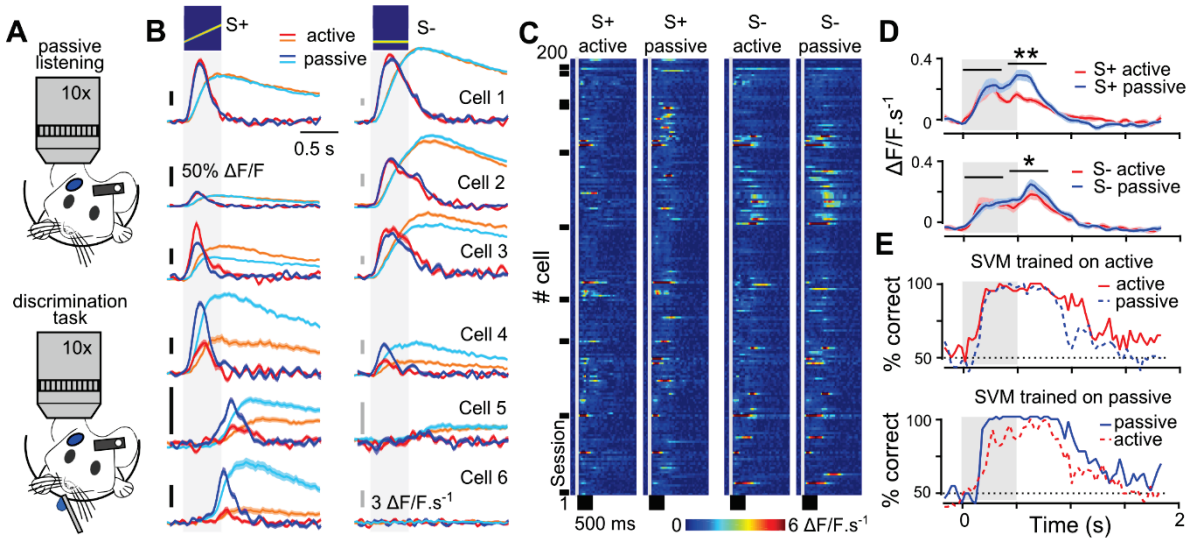

Figure S7, related to Fig. 6 | Stability of AC sound representations despite context-dependent modulations.A. Sketch of 2-photon imaging during passive listening and discrimination behavior. **B**. Traces of mean raw (light blue and orange) and deconvolved (blue and red) calcium signals for six example neurons. Cells 1 and 2 had similar responses in the active and passive states while cells 3 and 4 had boosted early responses in the active state and cells 5 and 6 diminished late responses during the active state (discrimination task). **C.** Heatmap showing mean deconvolved calcium signal to S+ and S- during the two different contexts for the 200 most responsive neurons (11 imaging sessions, 3 mice) for either sound and context (ranked by their p-value for the Wilcoxon signed rank test, n = 63 trials). **D**. Mean deconvolved signal for 1008 imaged neurons in response to S+ (top) and S- stimuli (bottom) during active and passive contexts. **E.** Discrimination performance of an SVM classifier trained with neuronal population activity (1008 neurons) during active (top) and passive context (bottom) and tested with both contexts.